Research Article

In vivo interictal signatures of human periventricular nodular heterotopia

Valerio Frazzini, MD, PhD,[1,2,3,*] Stephen Whitmarsh, PhD,[2,*] Katia Lehongre, PhD,[2] Pierre Yger, PhD,[4] Jean-Didier Lemarechal, PhD,[2] Bertrand Mathon, MD,[2,3,5] Claude Adam, MD, PhD,[1] Dominique Hasboun, MD, PhD,[2,3,6] Virginie Lambrecq, MD, PhD,[1,2,3] and Vincent Navarro, MD, PhD,[1,2,3†]

[1]AP-HP, Pitié Salpêtrière Hospital, Epilepsy Unit and Reference Center for Rare Epilepsies, F-75013, Paris, France

[2]Institut du Cerveau et de la Moelle épinière, ICM, INSERM, CNRS, F-75013, Paris, France

[3]Sorbonne Université, F-75013, Paris France

[4]Institut de la Vision, INSERM UMRS 968, UPMC UM 80, France

[5]AP-HP, Pitié Salpêtrière Hospital, Department of Neurosurgery, F-75013, Paris, France

[6]AP-HP, Pitié Salpêtrière Hospital, Department de Neuroradiology, F-75013, Paris, France

[*] Contributed equally to this study.

Corresponding author: Vincent Navarro

Corresponding author's address: Epilepsy Unit, Pitié-Salpêtrière Hospital, 47 boulevard de l'Hôpital, 75651 Paris cedex 13, France

Corresponding author's phone and fax: Tel: 33 1 42 16 19 40, Fax: 33 1 42 16 19 42

Corresponding author's e-mail address: vincent.navarro@aphp.fr

Running head: Signatures of periventricular heterotopia

Number of words in abstract: (100/100 words)

Number of words in main text: (1494/1500 words)

Number of figures: 3/3

Number of tables: 0

Number of supplementary figures: 2

Number of supplementary tables: 3

Acknowledgement statement

We would like to thanks Pierre Pouget (ICM, Pitié-Salpêtrière hospital, Paris, France) for the helpful discussions and comments on the manuscript.

Funding

This study was supported by the program “Investissements d’avenir” ANR-10-IAIHU-06, and grants from the OCIRP-ICM and the Fondation de l’APHP pour la Recherche - Marie-Laure PLV Merchandising.

Competing interests

The authors report no competing interests.

ABSTRACT (limit 100 words)

Periventricular nodular heterotopia (PNH) causes drug-resistant epilepsy. We analyzed *in vivo* interictal activities from three nodules of two epileptic patients using macro-microelectrodes. Two highly unusual interictal LFP patterns (IPs) were identified: Trains of periodic slow waves and isolated slow deflections, both with superimposed fast activity. These patterns were restricted to the nodules, and largely invisible on adjacent macroelectrodes. Neuron firing rates were significantly modulated during *all* IPs, suggesting that similar or overlapping neuronal populations generate different IPs. This study presents the first *in vivo* multi-level evidence of local PNH networks in humans and their organization into multiple interictal events.

INTRODUCTION

Periventricular nodular heterotopia (PNH) is a common type of cortical malformation.[1] PNH results from abnormal neuronal migration wherein gray matter forms nodular masses close to the walls of the lateral ventricles.[2] While PNH is associated with drug-resistant focal epilepsy, evidence of its intrinsic epileptogenicity is still lacking.[3,4]

Previous studies of other types of brain lesions have shown only a subset of neurons modifying their firing rate during the interictal events.[5-7] Moreover, only interictal spikes have been investigated. The goal of our study was to characterize the involvement of neurons during all interictal patterns (IPs) generated within human PNH. Furthermore, we investigated whether different IPs involve the same neuronal populations, or whether they involve different units and cell-types.

Three PNH nodules, from two patients, were recorded by means of combined macro-microelectrodes placed within the nodules. We identified two unusual but consistent LFP interictal signatures, in addition to epileptic spikes. Spike clustering of action potentials was used to identify putative single units, and their firing rates were time-locked to interictal events in the LFPs. Finally, a separation into pyramidal cells and interneurons was performed based on clustering of action potential morphology.

SUBJECTS/MATERIALS AND METHODS

SEEG recording

Patients gave written informed consent (project C11-16 conducted by INSERM and approved by the local ethic committee, CPP Paris VI). Two patients were implanted with bilateral intracranial depth electrodes (AdTech®) according to the clinical practice and the epilepsy features of the patients. Two (Patient 1) and three (Patient 2) Behnke-Fried type macro-micro electrodes were inserted (Fried et al., 1999). Post-implantation electrode locations were based on a pre-implantation 3T 3D-MRI, post-implant 1.5T 3D-MRI and CT scan, integrated using the Epiloc toolbox, an in-house developed plugin for the 3D-Slicer visualization software (Supplementary Table 1).[9,10]

Visual analysis of micro-LFP patterns

IPs were identified on the microelectrodes. Criteria for each pattern were then determined and used for a complete manual scoring of continuous data recorded at the first day after implantation. Patient 1 was analyzed for 24 hours. Patient 2, due to richness of interictal activity, was analyzed for 6 hours. Annotation of data was performed with software developed in-house (MUSE; supplementary material and methods).

Spectral analysis of micro-LFP patterns, Spike-Sorting and classification analysis

Analyses were performed with a combination of FieldTrip and custom MATLAB (The Mathworks Inc., Natick, Massachusetts) scripts.[11] A combination of density-based clustering and template matching algorithms were used to automatically cluster the detected spikes.[12] Resting behavior of detected units was further explored by the analysis of mean firing rate and Coefficient of Variation.[13] Finally, we classified detected units into putative pyramidal cells and interneurons, based on the half-width duration and trough-peak time of their waveforms (Supplementary material).[14]

RESULTS

Novel LFP epileptic activities revealed by microelectrodes

In both patients, seizures started at electrode contacts located in the PNH, with a secondary propagation to other cortical areas (Fig. 1J, K & Supplementary patient information). Three consistent IPs were recorded from microelectrodes: Periodic Slow Waves, Fast Activity and Epileptic Spikes (Fig. 1 & 2). These IPS were rarely visible on the macroelectrodes. Epoch-by-epoch correlations between the microelectrode and adjacent macroelectrode contacts showed that the IPs were only present in the macroelectrode contact, within the PNHs (Fig. 2 E, Supplementary Table 2).

Periodic Slow Waves

Periodic Slow Waves (PSW; Fig.1 C&F, right) were seen in both Nodule 1 (n=1882) and Nodule 2 (n=973). The periodicity of the PSW is apparent from the LFP averages in Nodule 1 (Fig. 2A, right) and Nodule 2 (Fig. 2B, right). Average (±σ) duration of a single slow wave was 283 (±74) ms in Nodule 1, and 271 (±72) ms in Nodule 2. Time periods between onset of two slow waves was 511 (±148) ms in Nodule 1, and 574 (±152) ms in Nodule 2. 83% (Nodule 1) and 79% (Nodule 2) of these time periods varied less than 25% from the average period, in accordance with periodicity. Low voltage fast activity (FA) was superimposed on the slow waves (Fig. 1C&F). Frequency analysis showed a mean peak at 112 Hz (Nodule 1) and 137 Hz (Nodule 2). These FA were clearly modulated in accordance with the periodicity of the slow waves.

Fast Activity

Isolated trains of Fast Activity (FA) were seen in both Nodule 1 (n=1005) and 2 (n=93). In Nodule 1, FA was usually superimposed on a polyphasic slow deflection (0.5s-1s, Fig. 1C, middle), while in Nodule 2, FA occurred at the onset of a sharply appearing slow deflection (2s-4s, Fig. 1F, middle). Time-frequency analysis showed that in Nodule 1, power increased to 43Hz and 96Hz for ≈ 0.5s during the FA (Fig. 2A, middle). Nodule 2 showed a clear narrow-band increase of power at 112Hz for at least 1s (Fig. 2B, middle). In Nodule 3, low amplitude deflections coincided with periodic short trains of fast activity (n=533), that lasted for 326 ± 79ms. Periods were 1075 ± 241ms (Fig. 1F), of which 91% varied less than 25% from the average period in accordance with periodicity. Time-frequency analysis showed clear periodic modulation of high frequency power, centered on 110Hz (Fig. 2D, right).

Epileptic Spikes

Epileptic Spikes (ES) were identified in all three nodules. Nodule 1 (n=3878) showed isolated sharp monophasic waves (Fig. 1C, left). In Nodule 2 (n=2705), spikes were generally followed (and often preceded) by a slow wave (Fig. 1F, left), which was also apparent in the average time-locked LFP (Fig. 2B, left). In Nodule 3 (n=403), spikes were characterized by a low amplitude di- or triphasic wave (Fig. 1I, left). Low voltage FA was superimposed on ES, with a mean peak at 113Hz, 137Hz and 126Hz, respectively (Fig. 2A-C, left).

All neurons are recruited by IPs

Spike clustering resulted in 25 units (Supplementary Table 3; Fig. 3D; Supplementary Fig. 1) of which 8 (32%) were classified as single units. Single units significantly modulate their firing rates in response to all interictal patterns: Firing-rate increased up to 505% for PSW, 4281% for FA, and 3840% for ES (Supplementary Table 3: ↑). Most of the units showed brief episodes of decreased firing rate surrounding the interictal activities, often by ≈ 100%, i.e. silence (Supplementary Table 3: ↓; Fig. 2 and Fig. 3A-C). Especially during ES, firing rates strongly decreased in all units within ≈ 500ms surrounding the discharge. Trial-by-trial correlations showed that the modulation of firing rates was highly consistent with the timing and shape of the interictal LFP in all units (Supplementary Table 3; Fig. 2; Fig. 3A-C). A massive increase of firing rate was shown for the very short duration of the ES, while FA was associated with a more prolonged increase of firing rate. During PSW, firing rates showed regular increases and decreases. Interestingly, three clusters, including 2 single units, significantly decreased their firing rate with respect to the IPs (Fig. 2C: middle panel; Supplementary Table 3: Nodule 2, Unit 4&5, and Nodule 3, Unit 2).

Exploratory classification of neuronal types

An exploratory classification of single units into neuronal types was based on the half-width and trough-to-peak time of the action potential (Fig. 3D). Putative interneurons and pyramidal cells were separated according to previous reports (Trough-to-peak: ≈ 0.5ms, Half-amplitude duration: ≈ 0.25 ms).[14] Seven out of 8 single units were classified as putative pyramidal cells, while one was consistent with a narrow-spiking putative interneuron (Fig. 3D). No clear differences were observed in neuronal firing behavior between principal neuron and interneurons (Supplementary Figure 2).

DISCUSSION

This study reports the first *in vivo* multi-level description of interictal epileptic neurophysiological patterns in human PNH. Two novel, highly consistent interictal LFP patterns (IPs) were identified: Periodic Slow Waves (PSW) and isolated slow waves with Fast Activity (FA). During these IPs, the modulations of neuronal firing rates were remarkably consistent, both within IPs, and across nodules, suggesting that these IPs provide a potential pathognomonic signature of PNH. Previous studies of cortical and mesial temporal IPs have shown heterogeneous patterns of neuronal firing during interictal spikes.[7,15,16] However, these studies did not investigate PNH, precluding the identification of consistent IPs within a specific type of lesion.

Interestingly, *all* spontaneously active neurons were shown to modulate their firing rate in accordance with *all* IPs. This suggests that similar neuronal populations can generate different interictal events based on the underlying network dynamics. Periodic IPs might occur as a response to alternating inhibition and rebound excitation.[17] During FA, increases of firing rates were more sustained than in the other patterns, while decreases in firing rate preceding the onset of FA, were less obvious. Epileptic spikes were clearly preceded by strong synchronous decreases in firing rate, followed by a short and rapid peaking in firing rate.

Finally, we found evidence for the involvement of both putative pyramidal cells and interneurons, in accordance with histological studies.[18,19] Neuronal types did not distinguish between interictal patterns, in line with our finding that the IPs involve the majority of the cell population.

To conclude, PSW and FA might provide a pathognomonic signature of PNH reflecting highly pathological network activity that recruits all spontaneously active neurons.

REFERENCES

1. Guerrini R, Dobyns WB. Malformations of cortical development: clinical features and genetic causes. Lancet Neurol 2014; 13(7), 710–726.

2. Dubeau F, Tampieri D, Lee N, Andermann E, et al. Periventricular and subcortical nodular heterotopia A study of 33 patients. Brain 1995; 118(5), 1273–1287.

3. Battaglia G, Chiapparini L, Franceschetti S, Freri E, et al. Periventricular Nodular Heterotopia: Classification, Epileptic History, and Genesis of Epileptic Discharges. Epilepsia 2006; 47(1), 86–97.

4. Valton L, Guye M, McGonigal A, Marquis P et al. Functional interactions in brain networks underlying epileptic seizures in bilateral diffuse periventricular heterotopia. Clin Neurophysiol 2004; 119(1), 212–223.

5. Wyler AR, Ojemann GA, Ward AA Jr. Neurons in human epileptic cortex: correlation between unit and EEG activity. Ann Neurol 1982; 11(3):301-8.

6. Ulbert I, Heit G, Madsen J, Karmos G, Halgren E. Laminar analysis of human neocortical interictal spike generation and propagation: current source density and multiunit analysis in vivo. Epilepsia 2004; 45 Suppl 4:48-56.

7. Keller CJ, Truccolo W, Gale JT, Eskandar E, et al. Heterogeneous neuronal firing patterns during interictal epileptiform discharges in the human cortex. Brain 2010; 133(6), 1668–1681.

8. Fried I, Wilson CL, Maidment NT, Engel J, et al. Cerebral microdialysis combined with single-neuron and electroencephalographic recording in neurosurgical patients. Technical note. J Neurosurg 1999; 91(4), 697–705.

9. Pérez-García F, Lehongre K, Bardinet E, Jannin P, Navarro V, Hasboun D, Fernandez-Vidal S. Automatic segmentation of depth electrodes implanted in epileptic patients: a modular tool adaptable to multicentric protocols. 31st International Epilepsy Congress 2015. (https://icm-institute.org/fr/cenir-stim-stereotaxy-core-facility-techniques-images-models/)

10. Fedorov A, Beichel R, Kalpathy-Cramer J, Finet J, et al. 3d Slicer as an image computing platform for the Quantitative Imaging Network. J Magn Reson Imaging 2012; 30(9), 1323–1341.

11. Oostenveld R, Fries P, Maris E, Schoffelen JM. FieldTrip: Open Source Software for Advanced Analysis of MEG, EEG, and Invasive Electrophysiological Data. Comput Intell Neurosci 2011; 1–9.

12. Yger P, Spampinato GL, Esposito E, Lefebvre B, et al. A spike sorting toolbox for up to thousands of electrodes validated with ground truth recordings in vitro and in vivo. eLife 2018; 7: e34518.

13. Shinomoto S, Shima K., Tanji J. Differences in spiking patterns among cortical neurons. Neural Computation 2003; 15(12), 2823–2842.

14. Bartho P, Hirase H, Monconduit L, Zugaro M, et al. Characterization of Neocortical Principal Cells and Interneurons by Network Interactions and Extracellular Features. J Neurophysiol 2004; 92(1), 600–608.

15. Le Van Quyen M, Bragin A, Staba R, Crepon B, et al. Cell type-specific firing during ripple oscillations in the hippocampal formation of humans. J Neurosci 2008; 28(24): 6104–6110.

16. Alvarado-Rojas C, Lehongre K, Bagdasaryan J, Bragin A, et al. Single-unit activities during epileptic discharges in the human hippocampal formation. Front Comput Neurosci 2013; 7: 140.

17. Tóth K, Hofer KT, Kandrács Á, Entz L, et al. Hyperexcitability of the network contributes to synchronization processes in the human epileptic neocortex. J Physiol 2018; 15; 596(2):317-342.

18. Thom M., Martinian L, Parnavelas JG, Sisodiya SM. Distribution of Cortical Interneurons in Grey Matter Heterotopia in Patients with Epilepsy. Epilepsia 2004; 45(8), 916–923.

19. Meroni A, Galli C, Bramerio M, Tassi L, et al. Nodular heterotopia: A neuropathological study of 24 patients undergoing surgery for drug-resistant epilepsy. Epilepsia 2009; 50(1), 116–124

FIGURE DESCRIPTION

Figure 1.

Electrodes implantation into the PNH nodules and interictal LFP patterns. (A, D & G) Brain MRI showing the electrodes trajectory, exploring the three analyzed nodules (A, Patient 1, nodule 1; D & G, Patient 2, Nodule 2 & 3). (B, E & H) schematic representation of the macro-microelectrodes (M1-M4: macroelectrode contacts; μ1-μ8: microelectrodes). All the geometrical features of the electrodes are expressed in millimeters. Macroelectrode recordings (C, F, I) are shown in bipolar montage. In nodule 1 (C) and 2 (F), three LFP patterns were recorded (Epileptic Spike, Fast Activity, Periodic Slow Wave). These patterns were apparent on microelectrodes (LFP μ1 and μ2), and to a smaller degree on macroelectrodes (M1-M2). LFP patterns were associated with MUA recorded on the microelectrodes. In nodule 3, two patterns were identified (I) that were apparent on the micro LFP, and to a smaller degree on macro LFP. (J,K) Examples of a seizure in Patient 1 and 2, showing seizure onset at deep electrode contact and microelectrodes located in periventricular nodules (* on time-axis denotes end of seizure in Patient 1).

Figure 2.

Time-locked LFP of interictal patterns in PNH and single neurons behaviors. Spike analysis shows similarities in pathological interictal patterns between PNH nodules (columns), and involvement of the same neuron in all patterns within nodules (rows). Top row in A-D shows average time-locked LFPs of patterns superimposed on an average time-frequency representation. Middle row in A-D shows rasterplots of spike times, time-locked to the patterns. Bottom row in A-D shows corresponding firing-rates, with clusters of significant change (yellow=increase, blue-decrease), compared to baseline (arrow). E) Correlations between LFP of micro- and macroelectrode contacts (bipolar montage) shows the strongest (positive = yellow) correlation with macroelectrode contacts closest to microelectrodes (marker-size = Pearson's ρ). Negative correlations (blue) show an inversion of dipoles for macroelectrode contacts further away from the microelectrodes. Size of markers scale with the absolute correlation (ρ).

Figure 3.

Characterization of single neurons features and behavior. Description of single unit behavior for Nodule 1 (A), Nodule 2 (B), and Nodule 3 (C), including template waveform, inter-spike-interval (ISI) histogram and firing-rates time-locked to

interictal patterns. Significant increases and decreases in firing-rate compared to baseline are indicated in yellow and blue, respectively. D) Unit classification. Trough-to-peak plotted against half-amplitude duration, resulting in two clusters of neuronal types. Pyramidal (Pyr) cells cluster on the top right, interneurons (Int) on the bottom-left. Filled symbols indicate single-unit activity (SUA), empty circus multi-unit activity (MUA). Average waveforms and 1000 overlaid responses show putative pyramidal cell (upside-down pyramid shape), and putative narrow-spiking inter-neuron (asterisk).

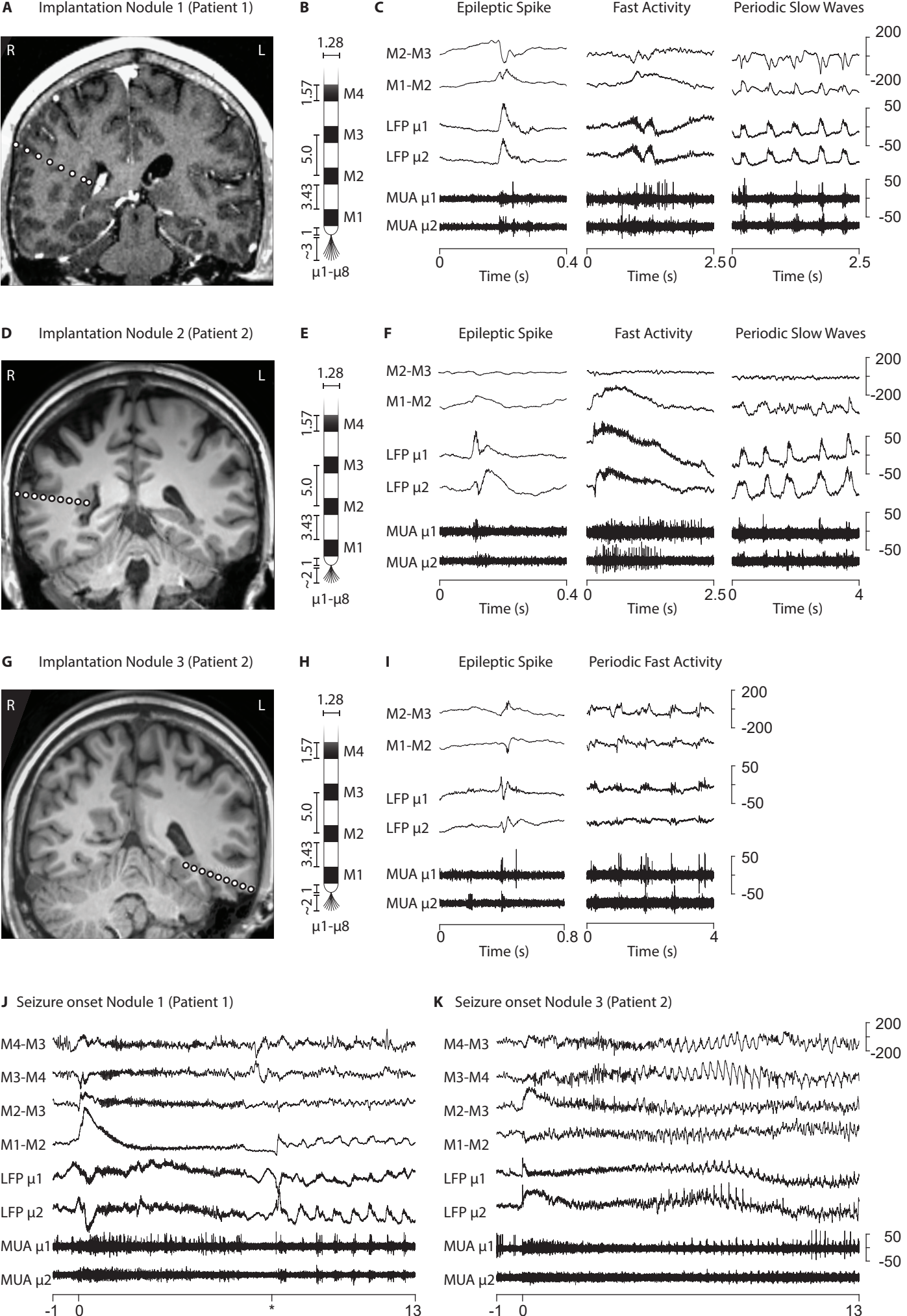
A
Implantation Nodule 1 (Patient 1)
R
L
B
1.28
1.57
5.0
3.43
~3.1
M4
M3
M2
M1
μ1-μ8
C
Epileptic Spike
Fast Activity
Periodic Slow Waves
M2-M3
M1-M2
LFP μ1
LFP μ2
MUA μ1
MUA μ2
200
-200
50
-50
0
0.4
2.5
Time (s)
D
Implantation Nodule 2 (Patient 2)
E
~2.1
F
4
G
Implantation Nodule 3 (Patient 2)
H
I
Periodic Fast Activity
0.8
J
Seizure onset Nodule 1 (Patient 1)
M4-M3
M3-M4
-1
13
K
Seizure onset Nodule 3 (Patient 2)

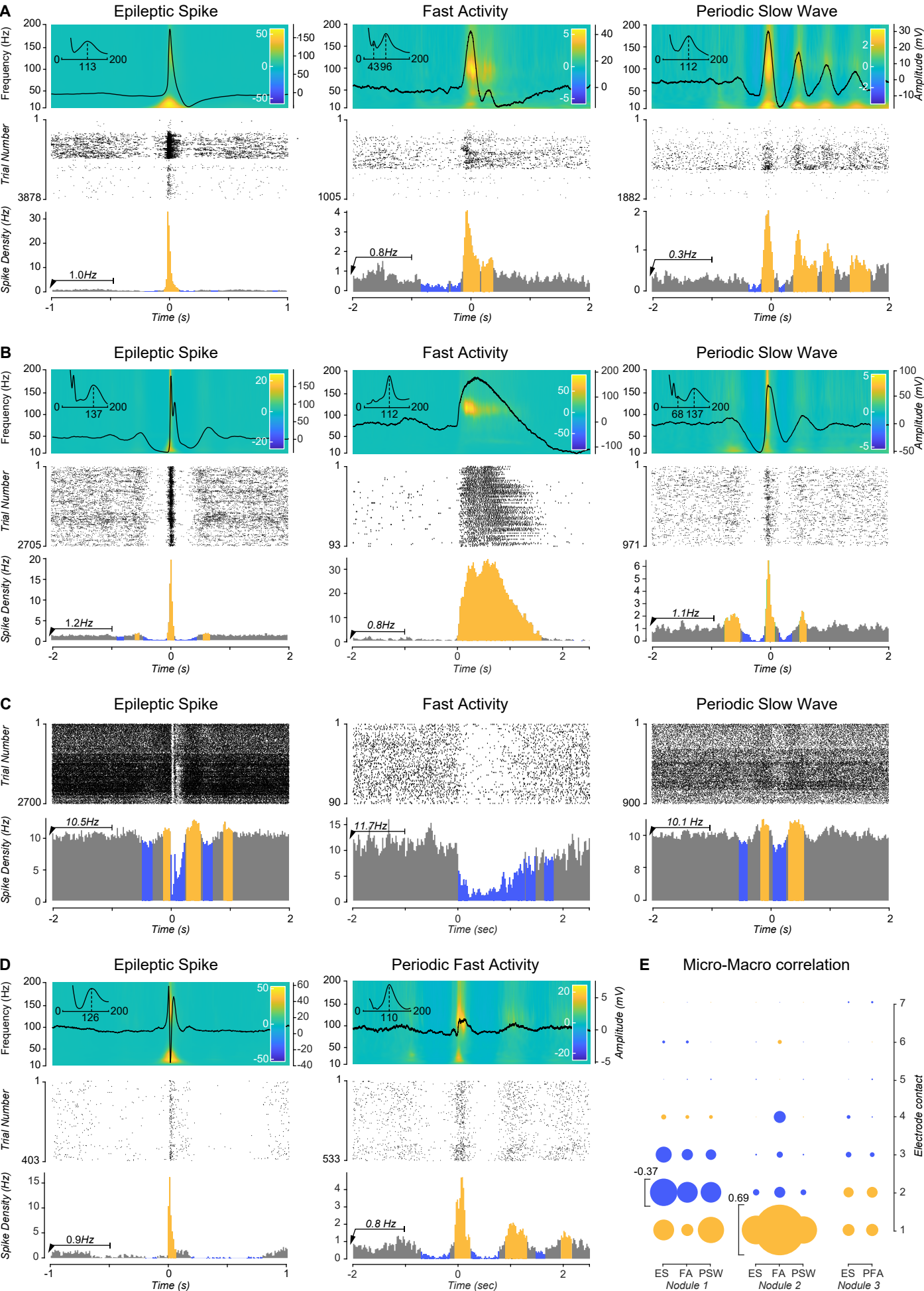
A
Epileptic Spike
Fast Activity
Periodic Slow Wave
Frequency (Hz)
Amplitude (mV)
Trial Number
Spike Density (Hz)
1.0Hz
0.8Hz
0.3Hz
Time (s)
B
Epileptic Spike
Fast Activity
Periodic Slow Wave
1.2Hz
0.8Hz
1.1Hz
C
Epileptic Spike
Fast Activity
Periodic Slow Wave
10.5Hz
11.7Hz
10.1 Hz
Time (sec)
D
Epileptic Spike
Periodic Fast Activity
0.9Hz
0.8 Hz
E
Micro-Macro correlation
Electrode contact
-0.37
0.69
ES FA PSW
Nodule 1
ES FA PSW
Nodule 2
ES PFA
Nodule 3

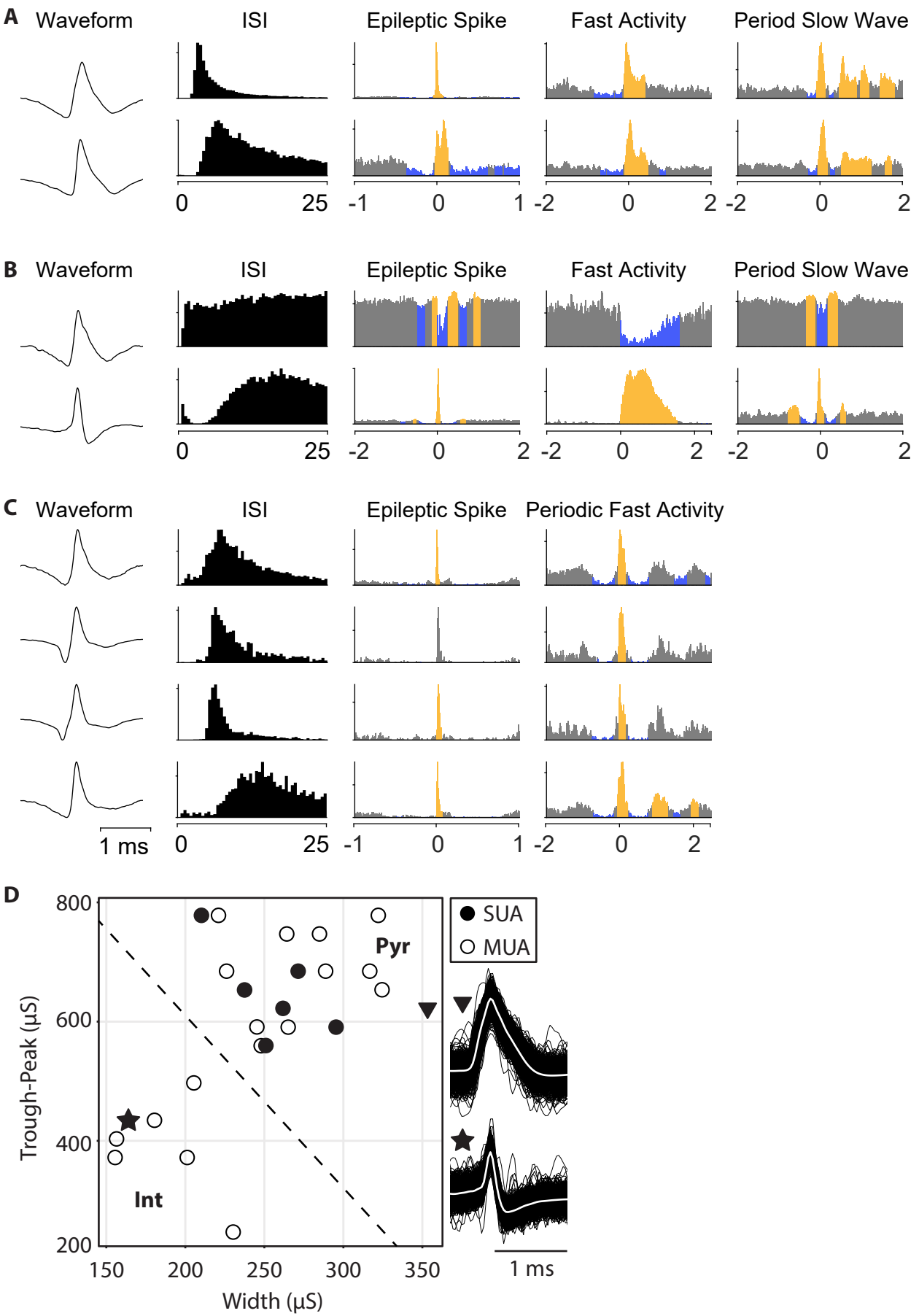
A
Waveform
ISI
Epileptic Spike
Fast Activity
Period Slow Wave
0
25
-1
0
1
-2
0
2
-2
0
2
B
Waveform
ISI
Epileptic Spike
Fast Activity
Period Slow Wave
0
25
-2
0
2
-2
0
2
-2
0
2
C
Waveform
ISI
Epileptic Spike
Periodic Fast Activity
1 ms
0
25
-1
0
1
-2
0
2
D
SUA
MUA
Pyr
Int
Trough-Peak (µS)
800
600
400
200
150
200
250
300
350
Width (µS)
1 ms